Magnetic anisotropy, interlayer coupling, and magneto-optical effects in single-crystalline Fe/Cr/Fe/MgO/Fe magnetotunnel structures grown on GaAs(001) substrates

J. Grabowski,[1] M. Przybylski,[1,a)] M. Nyvlt,[1,2] and J. Kirschner[1]
[1]*Max-Planck-Institut für Mikrostrukturphysik, Weinberg 2, 06120 Halle, Germany*
[2]*Institute of Physics, Faculty of Mathematics and Physics, Charles University, Ke Karlovu 5, 12116 Praha 2, Czech Republic*

(Received 29 July 2008; accepted 29 September 2008; published online 2 December 2008)

Fe/MgO/Fe single-crystalline magnetotunneling structures were epitaxially grown on GaAs(001). An independent magnetization switching in the Fe electrodes was achieved by pinning the magnetization of the Fe-top electrode by antiferromagnetic coupling across a Cr spacer to another Fe film. Such Fe/Cr/Fe/MgO/Fe/GaAs(001) structures exhibit in-plane anisotropy, which ensures a discrete switching behavior of magnetization simplifying the shape of the hysteresis loop. The field dependence of magnetization was measured along the [110] and [100] crystallographic directions of GaAs(001) substrate and modeled by minimizing the total magnetic energy of the system. A peculiar magneto-optical behavior (similar to a reversed hysteresis loop) is explained by magneto-optical phase angles, which are determined mainly by the optical properties of the semiconducting GaAs substrate. © *2008 American Institute of Physics*. [DOI: 10.1063/1.3021094]

I. INTRODUCTION

The magnetotunnel transistor (MTT) is one of the modern spintronic devices which was proposed recently.[1,2] MTT can be used to inject spin-polarized current into a semiconductor, which is a crucial issue for many devices combining new (spin) electronic with classical (charge)-semiconductor-based devices. An indicator of the performance of an MTT is the magnetocurrent ratio, which depends on the magnetization orientations of the emitter (top electrode of the junction) and the base (bottom electrode of the junction). Thus, a proper operation of the MTT requires an independent switching of magnetization of the emitter and of the base.

The combination of magnetic anisotropy and antiferromagnetic (AFM) interlayer coupling is interesting for applications because such systems are sensitive to magnetic fields along the easy axis of magnetization. The presence of in-plane anisotropy ensures a discrete switching behavior of magnetization simplifying the shape of the hysteresis loop, which depends on the ratio between the strength of the magnetic anisotropy and the strength of the AFM coupling.

We report on the in-plane magnetized single-crystalline Fe/Cr/Fe "artificial antiferromagnet" trilayers combined with the single-crystalline Fe/MgO/Fe magneto-tunnel junction (MTJ) structures grown on GaAs(001),[3] forming metal/insulator/metal/semiconductor structure of the MTT. Due to future applications, such as for the spin injection into the GaAs-based structure, the Fe/Cr/Fe trilayer is grown on top of the Fe/MgO/Fe/GaAs structure and pins the magnetization of the top electrode (emitter). Such Fe/Cr/Fe artificial antiferromagnet, if combined with the Fe/MgO/Fe MTJ, could remarkably improve the junction operation. The magnetization of one of the junction electrodes can be independently manipulated over a broad range of magnetic fields by a proper choice of the Cr spacer and Fe thicknesses in the Fe/Cr/Fe trilayer.[4]

The aim of the paper is to show how the electrodes magnetization can be manipulated by pinning one of them to an artificial antiferromagnet. The understanding of the magnetization reversal in the structure is found to be not trivial due to a complex interplay between the magnetic anisotropy, indirect interlayer coupling, and rather unusual magneto-optical effects.

II. EXPERIMENTAL ASPECTS

The GaAs substrates were prepared by preannealing to 520 °C, subsequent sputtering at the same temperature, and finally at 590 °C (with Ar ions of energy of 500 eV).[4] The growth of Fe, Cr, and MgO was carried out at a pressure below 4×10^{-10} mbar (maximum pressure after a long deposition of Fe).

To obtain the best MgO barriers, they were deposited at an elevated temperature (400 °C).[5] This allowed obtaining pinhole-free, atomically flat, and crystallographically well ordered insulating layers. The Fe/Cr/Fe structure was grown at room temperature. Low energy electron diffraction (LEED) patterns and high-resolution transmission electron microscopy (TEM) images confirm a good crystallographic order in the structures. The maximum thickness of the structure was 10 nm, which still satisfies the conditions of the ultrathin approximation.[6]

Magneto-optical Kerr effect (MOKE) ellipticity loops were collected for 1.85 eV photon energy (wavelength 670 nm) and incident *s*-polarized light at 49° to the sample normal using an electromagnet with maximum field of 30 mT. Due to the chamber limitations and construction details (a

a)Author to whom correspondence should be addressed. Tel.: +49 345 5582969. FAX: +49 345 5511223. Electronic mail: mprzybyl@mpi-halle.de.

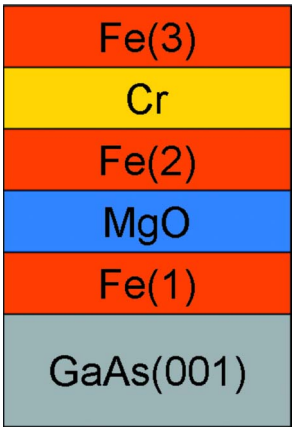

FIG. 1. (Color online) Schematic of the analyzed Fe/Cr/Fe/MgO/Fe/GaAs(001) structure.

magnet with a coil outside the chamber) the magnetic field was applied under an angle of 71.5° to the sample normal.

III. RESULTS

The Fe films grown on GaAs(001) at room temperature show a clear in-plane magnetic anisotropy. At low thickness, the uniaxial anisotropy of the easy axis along the [110] direction dominates over the fourfold anisotropy existing in the bcc-Fe(001) films. The anisotropy constants of the bottom Fe(1) layer (base of the MTT) depend on its thickness. We have grown the Fe(1) film 15 monolayer (ML) thick. For this thickness the fourfold anisotropy constant is similar to the uniaxial anisotropy constant.[7] Then the 10 ML thick layer of MgO was grown. The thickness was decided to separate magnetically both ferromagnetic electrodes of the junction.

On top of the MgO barrier we have grown Fe(3)/Cr/Fe(2) trilayers with a Cr thickness of 9 ML corresponding to AFM coupling between the Fe(3) and Fe(2) layers. The thickness of the bottom Fe(2) film (emitter of the MTT) was chosen to be exactly the same as of the Fe(1) film, i.e., 15 ML and was kept unchanged, whereas the thickness of Fe(3) was varied between 7 and 20 ML. The schematic diagram of the investigated structure is shown in Fig. 1.

At low fields, the Fe films in the Fe/Cr/Fe trilayer switch simultaneously and keep their AFM coupling. The switching field, H_c (coercivity of the trilayer), depends on the thickness relation between both Fe layers, i.e., the thickness of the thinner layer with respect to the thickness of the complete structure.[4] The lowest switching field obtained for the Fe/Cr/Fe trilayers with strongly different thicknesses of the Fe layers corresponds to the coercivity of the thicker layer and the highest is approached when the thickness of both Fe layers becomes similar. The switching field H_c depends on the direction along which the external magnetic field was applied.

The experimentally measured Kerr ellipticity hysteresis loops for the complete x ML Fe/9 ML Cr/15 ML Fe/10 ML MgO/15 ML Fe/GaAs(001) MTT-like structure are shown in Fig. 2. The loops were measured in the external magnetic field up to 30 mT only since it was the maximum field available in our experimental setup. The magnetic field was applied along two crystallographic directions of the GaAs(001) substrate: [110] (easy magnetization axis for Fe films thinner than 10 ML grown on GaAs(001) and [100] (easy magnetization axis of the Fe film grown on the MgO spacer layer). Only one parameter, i.e., the thickness of the Fe(3) layer, was varying; nevertheless, the measured loops are even qualitatively very different [compare Figs. 2(a) and 2(c)]. The shape of the loops can be explained as a superposition of the minor loop for the x ML Fe/9 ML Cr/15 ML Fe structure and a loop for the bottom 15 ML of Fe showing a small coercivity. The small coercivity loop corresponds to the bottom Fe(1) electrode, which behaves like a "free" Fe layer, i.e., magnetically separated from the top Fe/Cr/Fe structure. Net ellipticity is determined by a balance between different contributions of all Fe layers to the total MOKE signal.

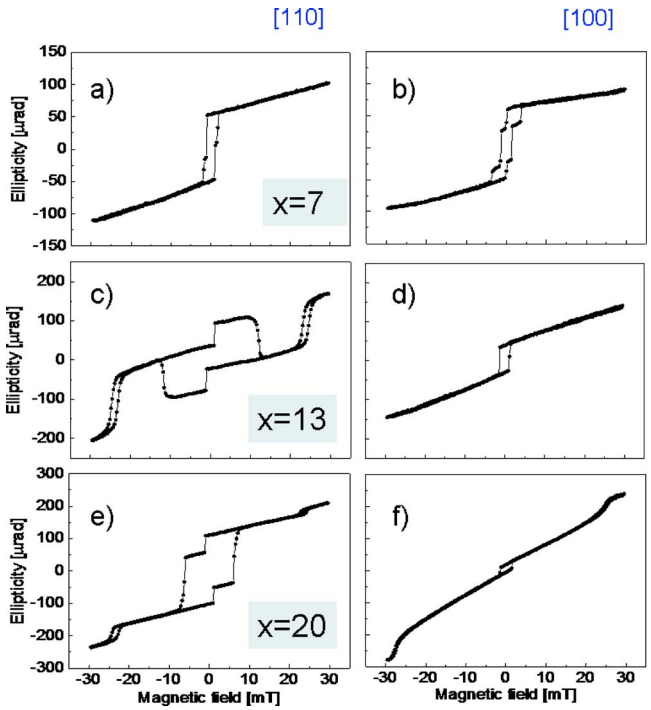

FIG. 2. (Color online) Longitudinal s-ellipticity MOKE loops measured along the [110] and [100] directions at room temperature for the Fe (x ML)/Cr (9 ML)/Fe (15 ML)/MgO (10 ML)/Fe (15 ML)/GaAs(001) structure with the thicknesses of the topmost Fe layer x=7, 13, and 20.

For d_3=7 ML, the loops measured both in the [110] and [100] are rather simple. The magnetization of the free Fe(1) layer and the top Fe(3)/Cr/Fe(2) structure switches almost at the same field [Fig. 2(a)]. A steplike loop along [100] is a result of steplike switching of the Fe/Cr/Fe magnetization, which switches at first to the [010] and then at a higher field to the [100] direction along which the field was applied [Fig. 2(b)].

The entire inclination of the ellipticity hysteresis loops in Fig. 2. is due to gradually increasing magnetization observed for the Fe(3)/Cr/Fe(2) trilayer and for the Fe(3)/Cr/Fe(2)/MgO/Fe(1) structure as a whole with increasing magnetic field. In part the inclination is caused by (a) the Fe(3)/Cr/Fe(2) trilayer of the net easy magnetization oriented along [100] direction, which follows the direction of the external magnetic field applied along [110], and (b) the Fe(1) layer of

the easy magnetization oriented along [110] direction, which follows the direction of the field applied along [100].

For $d_3=13$ ML, AFM coupling between the Fe layers of similar thickness ($d_2=15$ ML) in the Fe/Cr/Fe structure results in a H_c field of about 12 mT and in the spin-flop transition at about 25 mT when the field is applied along [110] [Fig. 2(c)]. The spin flop corresponds to more or less perpendicular orientation of the magnetization of the thinner Fe(3) film with respect to the magnetization of the thicker Fe(2) film, which is due to the interplay between magnetic anisotropy and interlayer magnetic coupling.[8] When the field is applied along the [100] direction, the magnetization of the Fe/Cr/Fe structure does not switch, i.e., H_c is above 30 mT [Fig. 2(d)]. This is not surprising since the thickness of Fe(3) and Fe(2) layers is almost the same and the magnetization in both cases is oriented along the easy magnetization axis.

The AFM-coupled Fe/Cr/Fe structure on GaAs(001) shows a peculiar magneto-optical behavior similar to a reversed hysteresis loop. Below the H_c-switching field, the thicker Fe(2) layer of the Fe(3)/Cr/Fe(2) structure is magnetized parallel to the applied field. The minor loop is reversed, i.e., a negative remanence is detected when the thicker bottom Fe(2) layer is magnetized along the applied field [Fig. 2(c)]. Only after the field is sufficient to invoke the spin-flop transition, the net ellipticity becomes positive.

With further increasing thickness of the top Fe(3) layer up to $d_3=20$ ML, the loop again changes the shape qualitatively. The magnetization of the Fe(3)/Cr/Fe(2) structure is imposed by the top Fe layer, which is now thicker than the bottom one ($d_2=15$ ML), and its magnetization follows the applied magnetic field. This is why the minor loop is no longer reversed [Fig. 2(e)]. The H_c-switching field is reduced due to the magnetization of the top Fe(3) layer dominating over the magnetization of the bottom one [Fe(2)]. Along the [100] direction, however, the switching at H_c is not visible up to the maximum applied field of 30 mT. Instead, a spin-floplike transition is observed at about 26 mT. Rather small intensity of the "free" Fe(1) layer is most likely due to relatively thick structure grown above this layer. This limits light penetration and causes the Fe(1) contribution to the total Kerr signal to be no more proportional to the film thickness.

IV. DISCUSSION

A. Magnetic anisotropy versus interlayer coupling

The coercivity H_c of the Fe(3)/Cr/Fe(2) depends on the relation between the thicknesses of both Fe layers. Note that in the case of $d_3=13$ ML and $d_3=20$ ML the ratio of the thickness of the thicker Fe film to the total thickness of both Fe films $(d_2/(d_2+d_3)=15/(15+13)=0.53)$ is not the same as for the case of the 20 ML Fe/9 ML Cr/15 ML Fe trilayer $[20/(20+15)=0.57]$. Therefore, H_c of the Fe/Cr/Fe trilayer is different in both cases changing from about 12 to 7 mT (compare Fig. 2).

The field values at which the magnetization changes, as well as the whole field dependence of magnetization $M(H)$, can be modeled by minimizing the total magnetic energy of the Fe(3)/Cr/Fe(2) system [the bottom Fe(1) layer was not included] including cubic (K_1) and in-plane uniaxial (K_u) anisotropies and both bilinear (J_1) and biquadratic (J_2) interlayer coupling

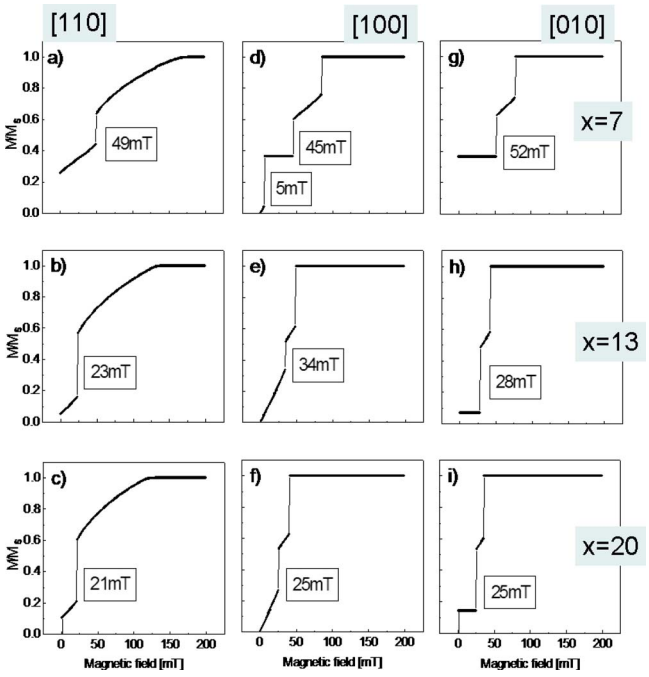

FIG. 3. (Color online) $M(H)$ curves calculated by minimization of the total magnetic energy for the Fe(3) (x ML)/Cr (9 ML)/Fe(2) (15 ML) trilayer with $x=7$, 13, and 20. The external magnetic field was assumed along three different crystallographic directions: [110], [100], and [010]. The anisotropy constants and exchange coupling constants taken for calculation are $K_1^{\mathrm{Fe}(2)}=K_1^{\mathrm{Fe}(3)}=4.5\times10^5$ erg/cm^3, $K_u^{\mathrm{Fe}(2)}=3\times10^4$ erg/cm^3, $K_u^{\mathrm{Fe}(3)}=4\times10^4$erg/cm^3, $J_1=0.11$ erg/cm^2, and $J_2=0.01$ erg/cm^2.

$$
\begin{aligned}
E(\Theta_{\mathrm{Fe}(3)},\Theta_{\mathrm{Fe}(2)}) = {} & HM_{\mathrm{Fe}(3)}\cos(\Theta_{\mathrm{Fe}(3)}-\Theta_H) \\
& + HM_{\mathrm{Fe}(2)}\cos(\Theta_{\mathrm{Fe}(2)}-\Theta_H) \\
& - (1/2)K_1^{\mathrm{Fe}(3)}(\cos^4\Theta_{\mathrm{Fe}(3)}+\sin^4\Theta_{\mathrm{Fe}(3)}) \\
& - (1/2)K_1^{\mathrm{Fe}(2)}(\cos^4\Theta_{\mathrm{Fe}(2)}+\sin^4\Theta_{\mathrm{Fe}(2)}) \\
& - K_{\mathrm{u}}^{\mathrm{Fe}(3)}\cos^2(\Theta_{\mathrm{Fe}(3)}-\Theta_u) \\
& - K_{\mathrm{u}}^{\mathrm{Fe}(2)}\cos^2(\Theta_{\mathrm{Fe}(2)}-\Theta_u) \\
& + J_1\cos(\Theta_{\mathrm{Fe}(3)}-\Theta_{\mathrm{Fe}(2)}) \\
& + J_2\cos^2(\Theta_{\mathrm{Fe}(3)}-\Theta_{\mathrm{Fe}(2)}).
\end{aligned}
$$

The external static magnetic field is applied in the plane of the film at an arbitrary angle Θ_H with respect to the cube axis. Θ_u is the uniaxial anisotropy direction. The magnetization angles $\Theta_{\mathrm{Fe}(3)}$ and $\Theta_{\mathrm{Fe}(2)}$ are measured with respect to the applied field direction. It is assumed that each layer is so thin that the magnetization is uniform across the film. The equilibrium magnetizations are constrained to rotate in the film plane. The calculated $M(H)/M_s$ curves (where M is the component of total magnetization along the field direction, which is then normalized to the saturation magnetic moment M_s) are shown in Fig. 3. The calculations were performed assuming the same fourfold anisotropy constants for both the Fe(3) and Fe(2) layers with the easy magnetization axis along the [100] direction and the fourfold anisotropy constant $K_1^{\mathrm{Fe}(2)}$

$=K_1^{Fe(3)}=4.5\times10^5$ erg/cm^3. However, in order to get a better agreement with the experimental data, it was necessary to assume additional uniaxial anisotropy with the easy magnetization axis oriented along the [010] direction and the anisotropy constant $K_u^{Fe(2)}=3\times10^4$ erg/cm^3 and $K_u^{Fe(3)}=4\times10^4$ erg/cm^3. It is not unusual that one of the ⟨100⟩ direction is easier than another one. This relates to the so called "growth anisotropy," which is most likely due to the geometry at which the films are grown. This kind of uniaxial anisotropy was already seen for a single Fe layer grown on the MgO buffer layer on GaAs(001).[9] The zero signal in this case corresponds to the magnetization oriented along the [010] direction, i.e., perpendicular to the external magnetic field applied along [100], which is the most preferable magnetization direction. For the $M(H)$ calculations, the saturation magnetization of Fe was assumed to be equal to 21 kOe. The exchange coupling constants used for the calculation were equal $J_1=0.11$ erg/cm^2 and $J_2=0.01$ erg/cm^2 for bilinear and biquadratic coupling, respectively, which are typical values for the Cr spacer 9 ML thick[10] and which reproduce the experimental hysteresis loops of the system the best. The calculations were performed for the external magnetic field applied along three different crystallographic directions: [110], [100], and [010].

The [010] direction was found to be the easiest one since it is forced both by fourfold and uniaxial anisotropies. The M/M_S values calculated along [010] at zero field provides an information on the magnetization orientation in both Fe layers in reference to the applied field. The calculations predict the spin-flop (or spin-floplike) change in magnetization of the Fe/Cr/Fe structure, e.g., at the field of 23 and 21 mT when applied along the [110] direction and the thickness of both layers (d_2 and d_3) does not differ too much [Figs. 3(b) and 3(c), respectively]. This is exactly the value that we experimentally measured for the Fe(3)/Cr/Fe(2) structure as shown in Figs. 2(c) and 2(e).

In particular, it is clear from the calculations that the energetically stable magnetization configuration persists up to a certain value when the field is applied along the [010] direction. The field value up to which the configuration is stable depends on how much the thickness of the Fe(3) layers differs from that of the Fe(2) layer {52, 28, and 25 mT for $d_3=7$, 13, and 20 ML, respectively [Figs. 3(c), 3(f), and 3(i)]}. At this field the magnetization of the thinner layer switches to the perpendicular orientation (i.e., along the [100] direction) and then gradually rotates toward [010]. Finally, the magnetization of the thinner layer switches to the orientation along the applied field, which is equivalent to the saturation of the Fe/Cr/Fe system.

When the field is applied along the [100] direction, the net magnetization increases from zero value at zero field by rotation toward the field direction and switching of both Fe(3) and Fe(2) magnetizations (not at the same field) to the final saturation configuration along the applied field [Figs. 3(e) and 3(h)]. The switching to the field direction below 30 mT is expected only for the Fe(3) layer $d_3=20$ ML thick, which is in agreement with the experimental result shown in Fig. 2(f). Only in the case of the thinnest Fe(3) film, i.e., for $d_3=7$ ML, the reversal process involves switching of both magnetizations at low field (5 mT) to the field direction, which results in a stable configuration up to the field of 45 mT [Fig. 3(b)]. Only then that the magnetization of thinner Fe(2) film switches at first to the [010] direction (spin-flop) and finally to the saturation configuration along the applied field. This is in full agreement with the experimental observation shown in Fig. 2(b).

In the case the external magnetic field is applied along the hard magnetization axis, i.e., along the [110] direction, the magnetization reversal proceeds in a different manner. A nonzero total magnetization value at zero field results from the projection of the [010] oriented magnetization to the [110] direction. Then the magnetization of the thinner Fe layer rotates toward the field direction and switches to the [100] direction, i.e., to the perpendicular orientation with the magnetization of the thicker Fe layer [spin-flop, Figs. 3(a), 3(d), and 3(g)]. The spin-flop transition below 30 mT is expected only for the Fe(3) film $d_3=13$ and 20 ML thick in agreement with experimental results shown in Figs. 2(c) and 2(e). Finally both the Fe(3) and Fe(2) magnetizations rotate to the field direction and the system saturates at the field of about 150 mT. The saturation field value remains in agreement with the previous observations for the Fe/Cr/Fe trilayers grown directly on GaAs(001).[4]

B. Magneto-optical properties

The reversed minor loop shown in Fig. 2 is explained by magneto-optical phase angles, which depend mainly on the optical properties of the substrate. The magneto-optical signals originating in the layers located in different depths of the ultrathin structure have different phases. Due to its placing inside the structure, the Fe(2) layer could contribute less to the total MOKE signal than the top (thinner) Fe(3) layer magnetized opposite to the field, which contributes with a negative ellipticity.[11] Consequently, the net ellipticity at positive fields could be negative. The thinner top Fe(3) layer could give a twice larger contribution to the longitudinal Kerr ellipticity than the thicker Fe located a few MLs deeper.[11]

This is important in the case of semiconducting substrates (like GaAs or Si), which produce the phases close to $-\pi$ (at least for the photon energy of our laser), i.e., to the phase where the magneto-optical ellipticity cancels. Then the layer for which the phase is closer to $-\pi$ contributes less to the overall ellipticity signal.[11] The calculations were performed within the matrix multilayer optical model employing the 4×4 matrix formalism[12] based on the electromagnetic theory of Maxwell and applied on absorbing structures.[13] The calculation details are described in Ref. 14. The Kerr phases could be precisely estimated also by the approximate formulas.[11] The calculations with both methods were carried out for the top layer (15 ML thick Fe film) of the Fe/Cr/Fe structure on a few different substrates. As seen from Fig. 4, the Kerr phase of the Fe layer when Fe/Cr/Fe is grown on GaAs is $\psi=-0.85\pi$ at the photon energy of 1.85 eV. The ellipticity angle $\varepsilon_j\approx-\Phi_j\sin\psi_j$, where Φ_j is called Kerr magnitude, is therefore very sensitive to small changes in ψ_j. It can happen that, as it is seen from Fig. 4, in the same

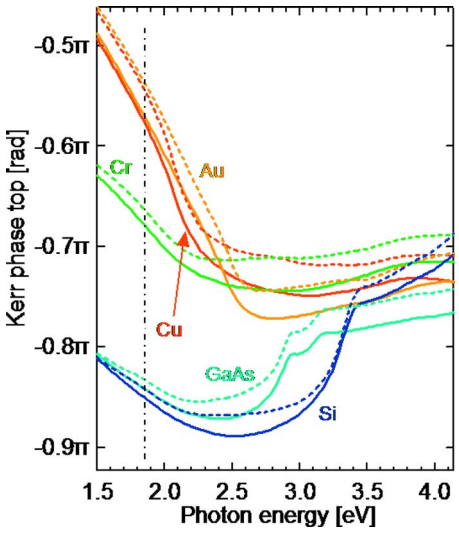

FIG. 4. (Color online) Kerr phase for the top Fe layer in the Fe(3)/Cr/Fe(2) structure grown on different metallic and semiconducting substrates calculated from the electromagnetic theory. Full lines correspond to the matrix multilayer optical model calculations (Ref. 13), whereas the dashed lines are obtained from the approximate formulas (Ref. 11).

Fe film when the Fe/Cr/Fe structure is grown on noble metals substrates, such as Cu or Ag, the typical values of the Kerr phase ψ_j are close to $-\pi/2$. In this case the ellipticity angle is not sensitive to the changes in ψ_j and accordingly the effect of reversed loops is not experimentally observed.

Individual contributions of all Fe layers of our particular system follow the predictions of the magneto-optical calculations in agreement with the MOKE results. Superconducting quantum interference device (SQUID) measurements confirm the interpretation of the MOKE loops. However, in agreement with the above consideration, $/\Phi_{\mathrm{Fe}(2)}/$ for $d_2=15$ ML is larger than $/\Phi_{\mathrm{Fe}(3)}/$ for $d_3=13$ ML. In the first approximation their ratio is $/\Phi_{\mathrm{Fe}(2)}/\Phi_{\mathrm{Fe}(3)}/\approx d_2/d_3$, but the Kerr phases cause $/\Phi_{\mathrm{Fe}(2)}\sin\psi_{\mathrm{Fe}(2)}/<\Phi_{\mathrm{Fe}(3)}\sin\psi_{\mathrm{Fe}(3)}/$ and one gets $/\varepsilon_{\mathrm{Fe}(2)}/<\varepsilon_{\mathrm{Fe}(3)}/$. Finally, since $\varepsilon_{\mathrm{Fe}(3)}$ is negative, it results in the negative net Kerr ellipticity and reversed minor loop.

For the Fe(3) layer $d_3=20$ ML thick, the magnetization of the Fe(3)/Cr/Fe(2) structure is dominated by the top Fe(3) layer, which is now quite thicker than the Fe(2) bottom one ($d_2=15$ ML), and its magnetization follows the applied magnetic field. This layer obviously contributes to the total MOKE signal with the positive ellipticity stronger than the negative contribution from the bottom Fe(2) layer magnetized opposite to the field direction. This is why the minor loop is no more reversed.

V. CONCLUSIONS

We have shown how complex hysteresis loops can be measured for single-crystalline MTJ structures combined with an artificial layer antiferromagnet pinning magnetization of one of the junction electrodes. The loops are interpreted by an interplay of rather complex magnetic anisotropy and indirect AFM exchange coupling between the Fe layers building up the artificial Fe/Cr/Fe antiferromagnet. It is shown how the magnetization reversal can be manipulated in the external magnetic field applied along three different crystallographic orientations. The effect of reversed loops is explained by the semiconducting substrate, which produces the phases close to $-\pi$. This could result in more contributions from the thinner than from the thicker Fe layer to the total ellipticity signal.

ACKNOWLEDGMENTS

The authors are very grateful to Professor B. Heinrich for providing us with the computer program to calculate the equilibrium magnetization directions.

[1] G. A. Prinz, Phys. Today **48**, 58 (1995).
[2] D. J. Monsma, J. C. Lodder, Th. J. A. Popma, and B. Dieny, Phys. Rev. Lett. **74**, 5260 (1995).
[3] J. Grabowski, M. Przybylski, M. Nyvlt, J. Zukrowski,W. Wulfhekel, J. Kirschner, J. Appl. Phys. **99**, 08C908 (2006).
[4] M. Przybylski, J. Grabowski, W. Wulfhekel, M. Rams, K. Tomala, and J. Kirschner, J. Appl. Phys. **95**, 597 (2004).
[5] M. Przybylski, J. Grabowski, F. Zavaliche, W. Wulfhekel, R. Scholz, and J. Kirschner, J. Phys. D **35**, 1821 (2002).
[6] J. Zak, E. R. Moog, C. Liu, and S. D. Bader, J. Magn. Magn. Mater. **88**, L261 (1990).
[7] M. Madami, S. Tacchi, G. Carlotti, G. Gubbiotti, and R. L. Stamps, Phys. Rev. B **69**, 144408 (2004).
[8] C. J. Gutierrez, J. J. Krebs, M. E. Filipkowski, and G. A. Prinz, J. Magn. Magn. Mater. **116**, L305 (1992).
[9] M. Przybylski, J. Grabowski, W. Wulfhekel, and J. Kirschner, Surf. Sci. **566–568**, 256 (2004).
[10] J. Unguris, R. J. Celotta, and D. T. Pierce, Phys. Rev. Lett. **67**, 140 (1991).
[11] Z. Q. Qiu, J. Pearson, and S. D. Bader, Phys. Rev. B **46**, 8195 (1992).
[12] P. Yeh, Surf. Sci. **96**, 41 (1980).
[13] S. Visnovsky, Czech. J. Phys., Sect. B **36**, 625 (1986).
[14] M. Nyvlt, M. Przybylski, J. Grabowski, and J. Kirschner, J. Appl. Phys. **98**, 033516 (2005).